



## Ultrasound assisted ambient temperature synthesis of ternary oxide $\text{AgMO}_2$ ( $M = \text{Fe}, \text{Ga}$ )

R. Nagarajan\*, Nobel Tomar

Materials Chemistry Group, Department of Chemistry, University of Delhi, Delhi 110 007, India

### ARTICLE INFO

#### Article history:

Received 13 November 2008

Received in revised form

29 January 2009

Accepted 30 January 2009

Available online 21 February 2009

#### Keywords:

Sonochemistry

Ion-exchange

Delafossites

### ABSTRACT

The application of ultrasound for the synthesis of ternary oxide  $\text{AgMO}_2$  ( $M = \text{Fe}, \text{Ga}$ ) was investigated. Crystalline  $\alpha\text{-AgFeO}_2$  was obtained from the alkaline solutions of silver and iron hydroxides by sonication for 40 minutes.  $\alpha\text{-AgFeO}_2$  was found to absorb optical radiation in the 300–600 nm range as shown by diffuse reflectance spectroscopy. The Raman spectrum of  $\alpha\text{-AgFeO}_2$  exhibited two bands at 345 and 638  $\text{cm}^{-1}$ . When  $\beta\text{-NaFeO}_2$  was sonicated with aqueous silver nitrate solution for 60 minutes,  $\beta\text{-AgFeO}_2$  possessing orthorhombic structure was obtained as the ion-exchanged product. The Raman spectrum of  $\beta\text{-AgFeO}_2$  showed four strong bands at 295, 432, 630 and 690  $\text{cm}^{-1}$ . Sonication of  $\beta\text{-NaGaO}_2$  with aqueous silver nitrate solution for 60 minutes resulted in olive green colored,  $\alpha\text{-AgGaO}_2$ . The diffuse reflectance spectrum and the EDX analysis confirmed that the ion-exchange through sonication was complete. The Raman spectrum of  $\alpha\text{-AgGaO}_2$  had weak bands at 471 and 650  $\text{cm}^{-1}$ .

© 2009 Elsevier Inc. All rights reserved.

### 1. Introduction

Ternary oxides with the chemical formula  $\text{ABO}_2$  exhibit different structural phases depending on the ionic size of  $A$  and  $B$  ions and their coordination preference. In the delafossite structure with a general formula  $\text{ABO}_2$ , the  $A$  cation (typically  $\text{Cu}^+$ ,  $\text{Ag}^+$ ,  $\text{Pd}^+$  and  $\text{Pt}^+$ ) is linearly coordinated to two oxygen ions; the  $B$  cation (typically  $\text{Fe}^{3+}$ ,  $\text{Ga}^{3+}$ ,  $\text{Cr}^{3+}$ ,  $\text{In}^{3+}$ ,  $\text{Co}^{3+}$ ) is located in a distorted  $\text{BO}_6$  octahedra sharing edges. It exhibits a layered structure in which a planar layer of ' $A$ ' cations in a triangular fashion are stacked alternatively with a layer of  $\text{BO}_6$  octahedra along the  $c$ -axis ( $\alpha$ -form). The delafossite structure can form two Polytypes,  $3R$  and  $2H$  depending on the orientation of each layer as shown in Fig. 1(a) and (b) with  $R\bar{3}m$  and  $P6_3/mmc$  space group symmetries, respectively. The orthorhombic modification of  $\text{ABO}_2$  ( $\beta$ -form) possesses the deformed wurtzite structure where in both the  $A$  and  $B$  cations are tetrahedrally coordinated to oxygen and crystallizing in the  $Pna2_1$  space group (Fig. 1(c)) [1–5]. The structural details of  $\alpha$ - and  $\beta$ -forms of the sodium and silver containing  $\text{ABO}_2$  oxides are listed in Table 1.

Though the existence of compound  $\text{CuFeO}_2$  with the delafossite structure is known since 1873, a series of papers by Shannon et al. [1–3] on the different synthetic strategies to prepare these compounds in powder as well as single crystal forms followed by the investigation of optical properties by Benko and Koffyberg [6–9] have identified these compounds to be technologically

important class of materials. The interest in the synthesis and properties of delafossite structured compounds grew immensely after the demonstration of p-type conductivity and optical transparency in the thin films of  $\text{CuAlO}_2$  by Kawazoe et al. [10].

The instability of Group I B metal oxides in the delafossite structure introduces many great challenges for the synthesis of these oxides. The delafossite structures containing silver have been prepared usually by low temperature synthesis techniques such as metathesis, high pressure, hydrothermal, oxidizing flux and cation exchange reactions [1–3,11,12]. Recently the syntheses of silver delafossites oxides have been excellently reviewed by Poeppelmeier et al. [13,14]. While Krauss [15] synthesized  $\alpha\text{-AgFeO}_2$  using  $\gamma\text{-FeOOH}$  and  $\text{Ag}_2\text{O}$  in a boiling  $\text{NaOH}$  solution at 100 °C, the same approach failed in case of other metal ions such as Ga, In etc. [14]. Unlike  $\text{Cu}^+$  ions which can disproportionate, aqueous ionic silver hydroxide species  $[\text{Ag}(\text{OH})_2]^-$  are stable at room temperature [13,14]. This stability has played a vital role in reducing the maximum temperature and the time required to form silver containing delafossites.

Sonochemical syntheses due to ultrasound irradiation are known to accelerate chemical reactions and initiate new reactions that are difficult to perform under normal conditions [16–18]. For example, the polymerization of polysiloxanes (silicones) has been accelerated with the aid of sonication. The sonochemical reactions of organometallics have been exploited as general approach for the synthesis of nanophase materials such as metals, alloys and carbides, metal sulfides, metal oxides, supported metal catalysts [16–18]. Recently, the work of Kim and Kim [19] on the use of ultrasound for the synthesis of nano-sized  $\text{LiCoO}_2$  from aqueous solutions of  $\text{LiOH}$  and  $\text{Co}(\text{OH})_2$  in flowing oxygen motivated us to

\* Corresponding author. Fax: +91 11 2766 6605.

E-mail address: [rnagarajan@chemistry.du.ac.in](mailto:rnagarajan@chemistry.du.ac.in) (R. Nagarajan).

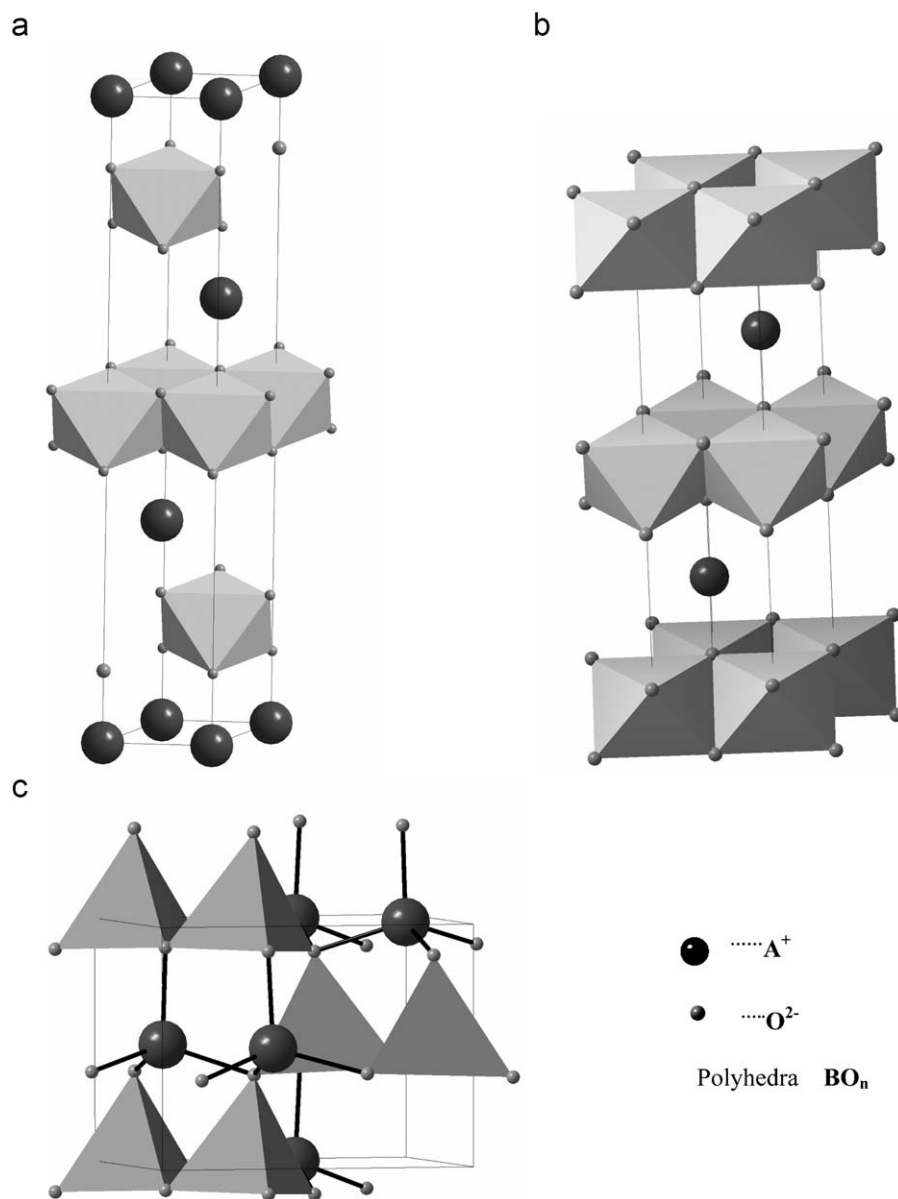


Fig. 1. (a) Delafossite structure (3R-polytype), (b) delafossite structure (2H-polytype) and (c)  $\beta$ -NaFeO<sub>2</sub> structure.

Table 1

Structural details of  $\alpha$ - and  $\beta$ -forms of AgMO<sub>2</sub> and NaMO<sub>2</sub> ( $M = \text{Fe, Ga}$ ).

Composition of oxides	Coordination class	Space group	$a(\text{\AA})$	$b(\text{\AA})$	$c(\text{\AA})$	Reference
$\alpha$ -AgFeO <sub>2</sub>	$A^{II}B^{VI}O_2^{IV}$	$R\bar{3}m$	3.039	3.039	18.595	JCPDS 25-0765
$\alpha$ -AgGaO <sub>2</sub>	$A^{II}B^{VI}O_2^{IV}$	$P6_3/mmc$	3.039	3.039	12.395	JCPDS 75-2147
$\beta$ -AgGaO <sub>2</sub>	$A^{IV}B^{IV}O_2^{IV}$	$R\bar{3}m$	2.9889	2.9889	18.534	1
$\beta$ -AgFeO <sub>2</sub>	$A^{IV}B^{IV}O_2^{IV}$	$Pna2_1$	5.563	7.149	5.471	JCPDS 21-1076
$\alpha$ -NaFeO <sub>2</sub>	$A^{VI}B^{IV}O_2^{IV}$	$Pna2_1$	5.635	7.105	5.547	JCPDS 21-1020
$\alpha$ -NaFeO <sub>2</sub>	$A^{VI}B^{IV}O_2^{IV}$	$R\bar{3}m$	3.022	3.022	16.08	JCPDS 82-1495
$\beta$ -NaFeO <sub>2</sub>	$A^{IV}B^{IV}O_2^{IV}$	$Pna2_1$	5.672	7.316	5.377	JCPDS 74-1351

investigate the use of ultrasound irradiation for the synthesis of silver containing ABO<sub>2</sub> ternary oxides in an open system. It is note worthy that LiCoO<sub>2</sub> exhibits  $\alpha$ -NaFeO<sub>2</sub> structure at high temperatures and pseudo spinel structure at low temperatures.

In the present study, we have investigated the synthesis of AgMO<sub>2</sub> ( $M = \text{Fe, Ga}$ ) with the help of ultrasound irradiation. The

choice of Fe<sup>3+</sup> and Ga<sup>3+</sup> for the B-site cation has been made for the following reasons: (i) the rate of the reaction of Ag<sub>2</sub>O with FeOOH to yield AgFeO<sub>2</sub> was found to increase with increase in hydroxide concentration in boiling NaOH [14], (ii) high solubility of gallate ion to yield 3R AgGaO<sub>2</sub> at the lowest temperature as compared to all other delafossite oxides under hydrothermal conditions [13,14]

and (iii)  $\alpha$ - and  $\beta$ -forms of  $\text{AgGaO}_2$  were found to be good visible light photocatalyst [20]. From the present investigation, ultrasound has been established to significantly accelerate the formation of  $\alpha$ - $\text{AgFeO}_2$  from the hydroxides of silver and iron as well as the ion-exchange reactions of  $\text{NaMO}_2$  ( $M = \text{Fe, Ga}$ ) with aqueous  $\text{AgNO}_3$  at room temperature.

## 2. Experimental

### 2.1. Synthesis

Equimolar solutions of  $\text{AgNO}_3$  (Rankem, 99%) and  $\text{Fe}(\text{NO}_3)_3 \cdot 9\text{H}_2\text{O}$  (Thomas Baker, 99%) were added to a solution of  $\text{KOH}$  (5 M) under constant stirring. The precipitated hydroxides were then subjected to sonication in a Round Bottom flask at powers 16.5 and 33 KHz for various intervals of time. For the ion-exchange studies, the parent compounds  $\text{NaMO}_2$  ( $M = \text{Fe, Ga}$ ) were prepared according to the procedure described in the literature [20]. The  $\text{NaMO}_2$  ( $M = \text{Fe, Ga}$ ) powders were then suspended in a twofold excess molar aqueous solution of  $\text{AgNO}_3$  (Rankem 99%) in a 250 ml RB flask and subjected to sonication at powers 16.5 and 33 KHz for various intervals of time.

### 2.2. Characterization

The powder X-ray diffraction patterns of the products were recorded using PANalytical X'Pert Pro diffractometer fitted with secondary graphite monochromator and employing  $\text{CuK}\alpha$  radiation. The UV–vis diffuse reflectance spectra of the powder samples with reference to  $\text{BaSO}_4$  powder were collected on Perkin Elmer spectrophotometer lambda 35 equipped with integrating sphere attachment. FT Raman Spectrum were obtained using a Renishaw–Raman spectrophotometer using 512 nm laser. SEM and EDAX analysis were carried out using FEI (Model QUANTA 200 FEG) energy dispersive X-ray system.

## 3. Results and discussion

The solution containing the hydroxides of silver and iron, when subjected to sonication at 16.56 KHz for 40 minutes, resulted in the formation of a brick red colored solid. The powder X-ray diffraction pattern of the solid confirmed it to be the delafossite structured  $\alpha$ - $\text{AgFeO}_2$  (Fig. 2(a)). The (00 $l$ ) reflections were intense suggesting the preferred orientation of the grains along the  $c$ -axis. The presence of the stacking disorder between the 2H and 3R polytypes along the  $c$ -axis was also revealed from the broadness of the peaks diffracted from the crystallographic planes neither perpendicular nor horizontal to the  $c$ -axis [20]. The broadness of the peaks may also be due to weakly crystalline nature of the product. The increased ultrasound power, viz., 33 KHz for the same duration did not remarkably influence the nature of the product except the fact that sharp (00 $l$ ) reflections became broader (Fig. 2(b)), suggesting a decrease in the crystallite size of the product with increased ultrasonic power. The average crystallite size of the product using Scherrer analysis yielded around  $\sim 9$  nm. However, the SEM image of  $\alpha$ - $\text{AgFeO}_2$  showed agglomeration of particles (Fig. 3(a)) and the EDX analysis showed the ratio of Ag: Fe to be 1:1 (Fig. 3(b)). As can be seen in the Fig. 2(b), the broadness of peaks masks the differences in the positioning of the peaks due to 2H and 3R polytypes. The refined lattice parameters considering the 3R-polytype were found to be,  $a = 3.060(9)\text{Å}$ ,  $c = 18.62(3)\text{Å}$ , as the positioning of peaks was matching more towards the 3R-polytype. The diffuse reflectance spectrum of the  $\alpha$ - $\text{AgFeO}_2$  powder was collected to quantify the

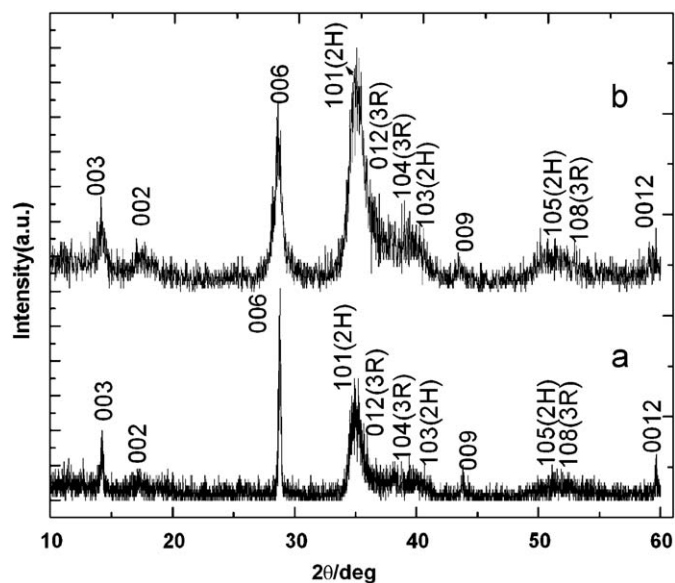


Fig. 2. Powder X-ray diffraction pattern of  $\alpha$ - $\text{AgFeO}_2$  obtained by the sonication of silver and iron hydroxides using: (a) 16.5 KHz and (b) 33 KHz for 40 minutes.

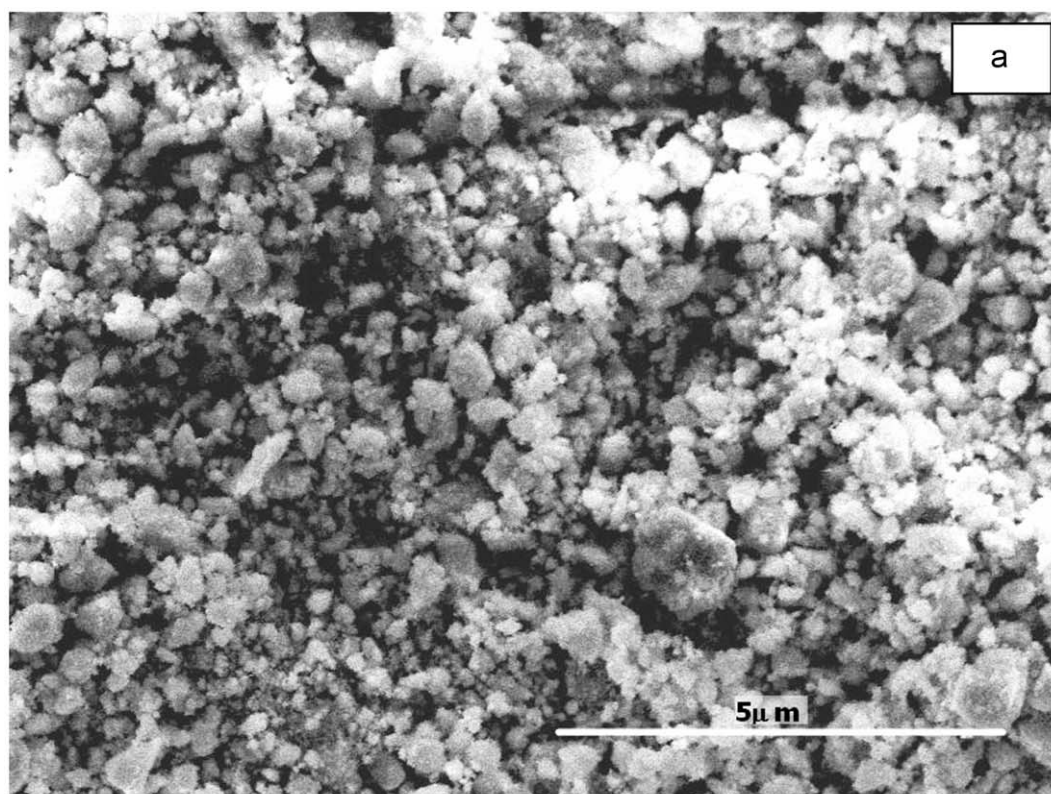
optical properties. The optical absorption for the samples was obtained by converting the diffuse reflectance data by Kubelka–Munk method. The  $\alpha$ - $\text{AgFeO}_2$  showed broad absorption in the 300–600 nm range (Fig. 4(a)) as reported for other silver containing delafossite structured oxides [13].

Raman spectroscopy has been extensively employed to effectively analyze the symmetry present in the crystalline materials. Few limited studies on the Raman spectrum of delafossite structured  $\text{CuCrO}_2$  and  $\text{PdCoO}_2$  have reported the presence of two bands in the 300–700  $\text{cm}^{-1}$  range [22–24]. Delafossite structure has four atoms in the unit cell, giving rise to 12 vibration modes. The reduction of the reducible representation  $\Gamma$  into the irreducible representations of the unit cell group is given by

$$\Gamma = 1A_{1g} + 3A_{2u} + 1E_g + 3E_u$$

Raman spectrum of delafossite structured  $\alpha$ - $\text{AgFeO}_2$  also showed two bands at 345 and 638  $\text{cm}^{-1}$  (Fig. 4(b)). The  $A$  modes imply the movement along the direction of the Ag–O bonds (i.e. along the hexagonal  $c$ -axis) whereas doubly degenerate  $E$  modes describe vibrations in the direction perpendicular to the  $c$ -axis. The existence of an inversion center in the delafossite structure could classify the normal modes in terms of their parity. The odd modes, denoted with the ‘ $u$ ’ subscript, are the acoustic modes ( $A_{2u}+E_u$ ) which are IR active. The two Raman active modes observed at 345 and 638  $\text{cm}^{-1}$  for  $\text{AgFeO}_2$  could be assigned to  $E_g$  and  $A_{1g}$  (Fig. 4(b)). Of these, the  $A_{1g}$  mode corresponded to the Fe–O stretching of  $\text{FeO}_6$  octahedra and the  $E_g$  mode to the O–Fe–O bending. This assignment was based on the fact that the movement of oxygen atoms attached to the central metal atom viz., Fe, was responsible for the observed Raman modes.

The preparation of  $\alpha$ - and  $\beta$ -modifications of  $\text{AgFeO}_2$  from  $\alpha$ - and  $\beta$ - $\text{NaFeO}_2$  through ion-exchange with molten  $\text{AgNO}_3$  has been reported in the literature [25]. The  $\beta$ - $\text{NaFeO}_2$  prepared by the well established procedures in the literature [20] showed an orthorhombic structure in the powder X-ray diffraction pattern (Fig. 5(a)). The ion-exchange of  $\beta$ - $\text{NaFeO}_2$  with aqueous  $\text{AgNO}_3$  was performed with the assistance of ultrasound to examine



c:\edax32\genesis\genmaps.spc 04-Sep-2008 17:23:08  
 < Pt. 1 Spot > LSecs : 7

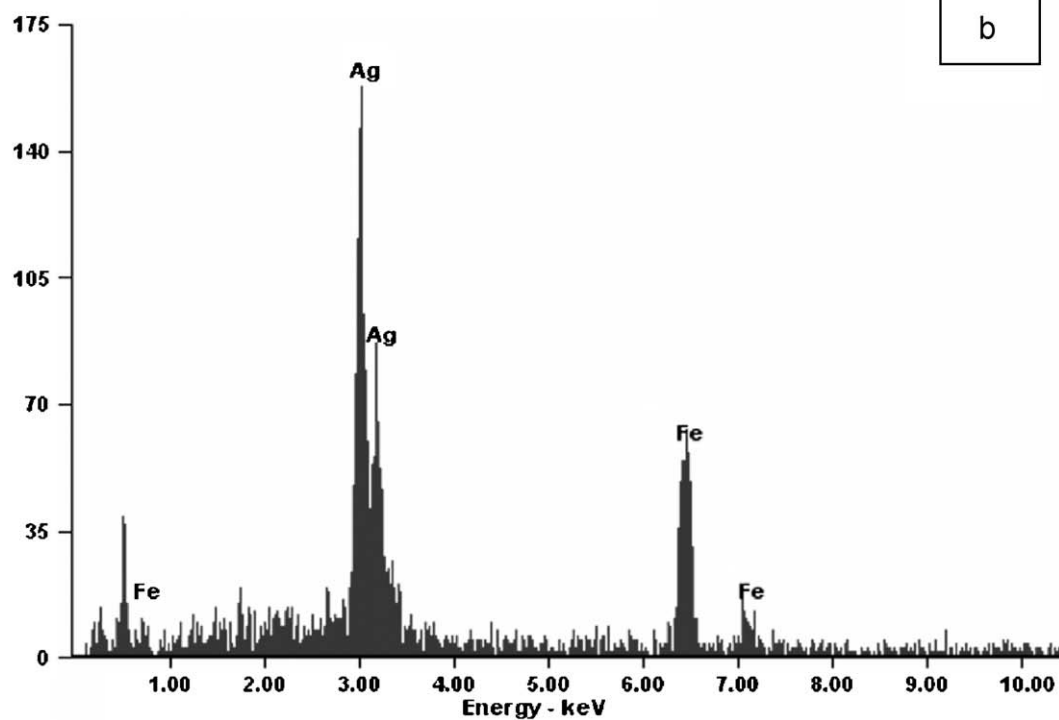


Fig. 3. (a) SEM image of  $\alpha$ -AgFeO<sub>2</sub> and (b) EDX spectrum of  $\alpha$ -AgFeO<sub>2</sub>.

whether  $\beta$ -AgFeO<sub>2</sub> is obtained. In a 100 ml RB flask,  $\beta$ -NaFeO<sub>2</sub> (0.744 g) powder was suspended in 20 ml of double distilled water containing 2.27 g of AgNO<sub>3</sub> and was subjected to sonication at 33 KHz at ambient temperature. After 60 minutes of sonication, a brick red colored solid was obtained. The peaks in the powder

X-ray diffraction pattern of the product matched very well with  $\beta$ -AgFeO<sub>2</sub> JCPDS File No. 21-1080 (Fig. 5(b)). The refined lattice parameters were  $a = 5.687(6)$ ,  $b = 7.162(9)$  and  $c = 5.597(8)$  Å. The average crystallite size using the Scherrer analysis yielded ~50 nm. The complete ion-exchange was further established from

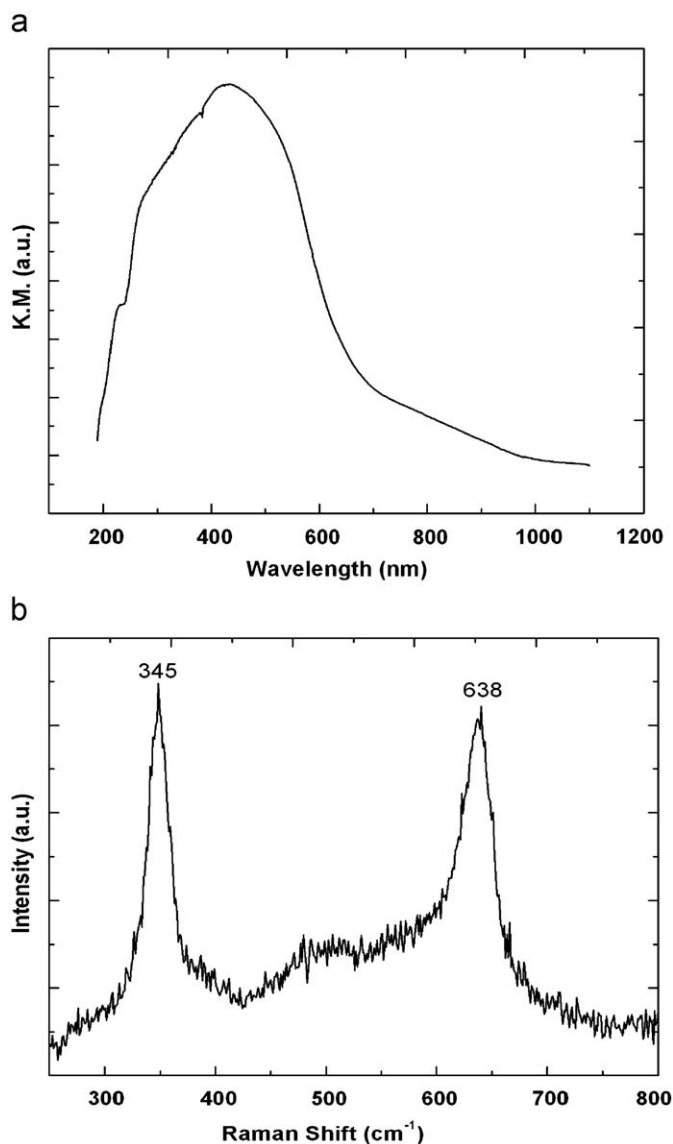


Fig. 4. (a) UV-vis diffuse reflectance spectrum of  $\alpha$ -AgFeO<sub>2</sub> and (b) Raman spectrum of  $\alpha$ -AgFeO<sub>2</sub>.

the SEM/EDX analysis of the product which showed the absence of sodium as well as the presence of Ag and Fe in the ratio 1:1 (Fig. 6(a) and (b)).

Both  $\beta$ -NaFeO<sub>2</sub> and  $\beta$ -AgFeO<sub>2</sub> showed broad absorption in the 200–600 nm range in the diffuse reflectance spectrum (Fig. 7(a)) as observed for the orthorhombic AgAlO<sub>2</sub> [26]. In the orthorhombic  $\beta$ -AgFeO<sub>2</sub>, there are four formula units per unit cell and  $C_{2v}$  is the corresponding point group of the  $Pna2_1$  space group. In this point group, all the four vibrational modes viz.,  $A_1(z)$ ,  $A_2$ ,  $B_1(x)$  and  $B_2(y)$  are Raman active. In the Raman spectrum of  $\beta$ -AgFeO<sub>2</sub>, four strong bands were observed with one weak band showing the presence of splitting (Fig. 7(b)). This band may be assigned to a totally symmetric stretching mode ( $A_1$ ) [27]. To the best of our knowledge, this is the first report of the Raman spectrum of  $\beta$ -AgFeO<sub>2</sub>.

The orthorhombic  $\beta$ -NaFeO<sub>2</sub> structured compounds have been found to be thermodynamically unstable at room temperature, however do not transform into the stable  $\alpha$ -modification because of kinetic reasons [21]. Often, hydrothermal treatment at 350 °C was found to be effective for the transformation [14,25]. After realizing the versatility of sonication in effectively transforming

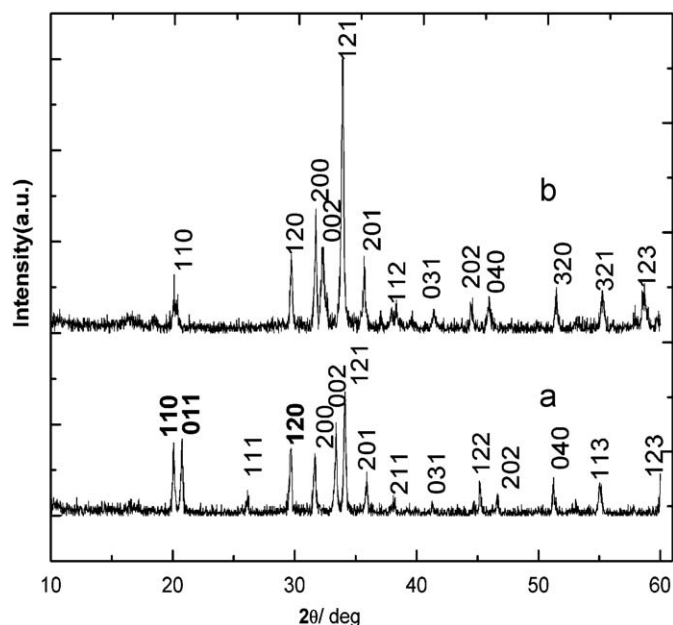
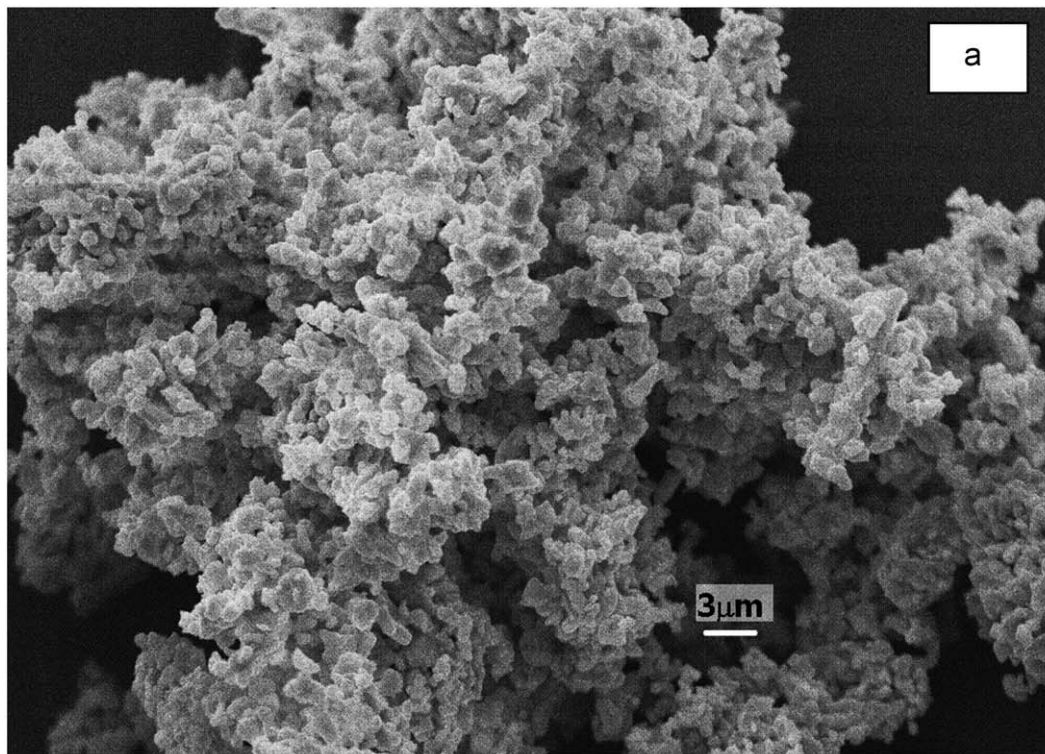


Fig. 5. Powder X-Ray diffraction patterns of: (a)  $\beta$ -NaFeO<sub>2</sub> and (b)  $\beta$ -AgFeO<sub>2</sub> obtained by ion-exchange using sonication.

the  $\beta$ -NaFeO<sub>2</sub> to  $\beta$ -AgFeO<sub>2</sub> at room temperature, its applicability in case of  $\beta$ -NaGaO<sub>2</sub> with aqueous AgNO<sub>3</sub> was examined. The aqueous solution containing AgNO<sub>3</sub> (0.70 g) and  $\beta$ -NaGaO<sub>2</sub> (0.25 g) solid was sonicated (33 KHz) in a 100 ml round bottom flask for about 60 minutes at room temperature. The white color, originally present, was gradually changed to yellow on sonication. The solid turned to olive green in color towards completion.

The powder X-ray diffraction pattern of the olive green colored product indicated the formation of  $\alpha$ -AgGaO<sub>2</sub> (Fig. 8(a) and (b)). In the delafossite structured  $\alpha$ -AgGaO<sub>2</sub>, only 3R-polytype has been synthesized in pure form [1]. The refined lattice parameters, considering the 3R-polytype, for our preparation were  $a = 2.997(7)$  Å,  $c = 18.56(2)$  Å. The transformation of  $\beta$ -AgGaO<sub>2</sub> to  $\alpha$ -AgGaO<sub>2</sub> was reported earlier using hydrothermal [1–3,25] or by stirring in hot water for longer duration [20]. The presence of aqueous medium along with the ultrasonic waves in the present study might be the driving force for the conversion of  $\beta$ -phase to  $\alpha$ -phase. The peaks in the powder X-ray diffraction pattern (Fig. 8(b)) were broader as in the case of  $\alpha$ -AgFeO<sub>2</sub>. The average crystallite size was  $\sim 5$  nm from Scherrer analysis. The UV-vis diffuse reflectance spectrum of  $\alpha$ -AgGaO<sub>2</sub> (Fig. 9(a)) showed a shift in the absorption edge to the visible range which matched well with the reported data in the literature [13]. The formation of delafossite phase was further supported by the Raman spectrum of  $\alpha$ -AgGaO<sub>2</sub> which showed the two characteristic bands at 471 and 650 cm<sup>-1</sup>. These bands could be assigned to the bending and stretching vibrations of the metal–oxygen in an octahedral environment, viz., the  $E_g$  and  $A_{1g}$  modes, respectively (Fig. 9(b)). The broadening of Raman bands observed may be due to the oxygen deficiency in the sample and smaller grain size of  $\alpha$ -AgGaO<sub>2</sub>. This procedure of direct conversion of  $\beta$ -NaGaO<sub>2</sub> to  $\alpha$ -AgGaO<sub>2</sub> with the assistance of ultrasonic treatment can be described as ‘one-pot synthesis’. The SEM image of  $\alpha$ -AgGaO<sub>2</sub> prepared by this procedure is shown in Fig. 10.

The following are the underlying facts of a chemical reaction assisted by ultrasonic waves in aqueous medium. The formation, growth and implosive collapse of bubble in an ultrasonically irradiated liquid, generates transient localized ‘hot spots’ with an effective temperature of 5000 K, pressures of  $>20$  MPa having a



c:\ledax32\genesis\genmaps.spc 04-Sep-2008 17:26:18  
 <Pt. 1 Spot> LSecs : 8

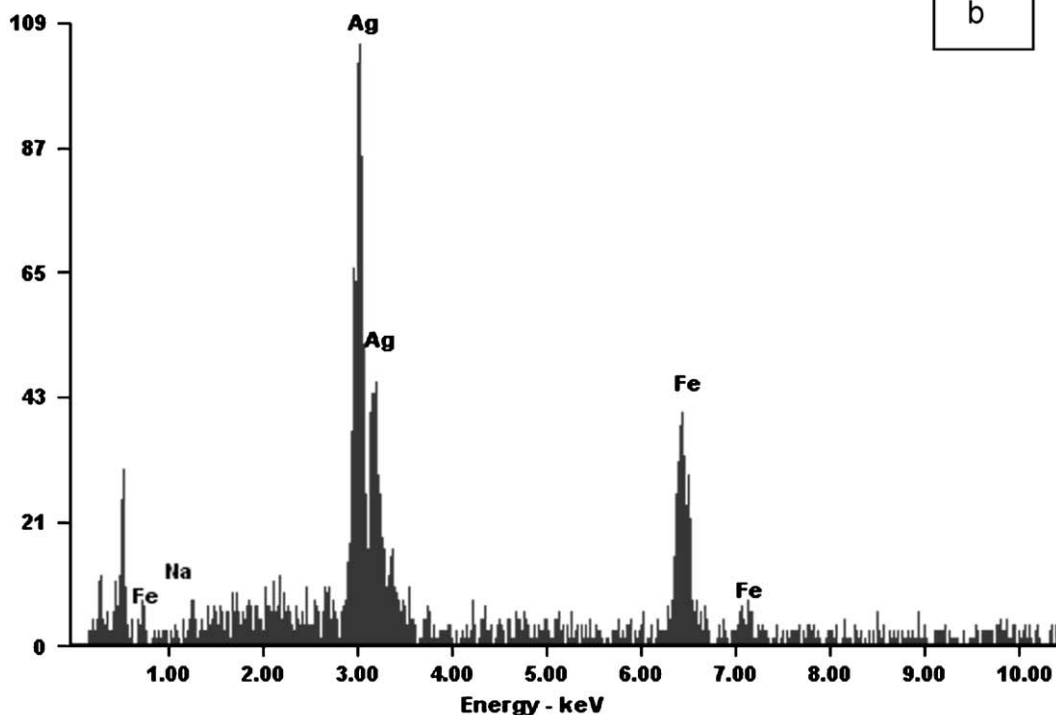


Fig. 6. (a) SEM image of  $\beta$ -AgFeO<sub>2</sub> and (b) EDX spectrum of  $\beta$ -AgFeO<sub>2</sub>.

nanosecond lifetime with a rapid cavitation cooling rate ( $> 10^9$  K/second) [28,29]. Moreover, in a solid–liquid system, when a bubble collapses near an extended surface, it causes high velocity interparticle collisions leading to fragmentation and thus substantially increasing the available surface area of powders enhancing the reaction rate in layered inorganic solids [30,31]. One of the most pertinent effects of ultrasound on liquid–solid

system is mechanical in nature and attributed to symmetric and asymmetric cavitations which have the potential of creating microscopic turbulence within interfacial films surrounding nearby solid particles. This micro-streaming phenomenon increases the rate of mass transfer of reactants across the solid–liquid film, thus increasing the intrinsic mass transfer coefficient as well as thinning the film [19,32].

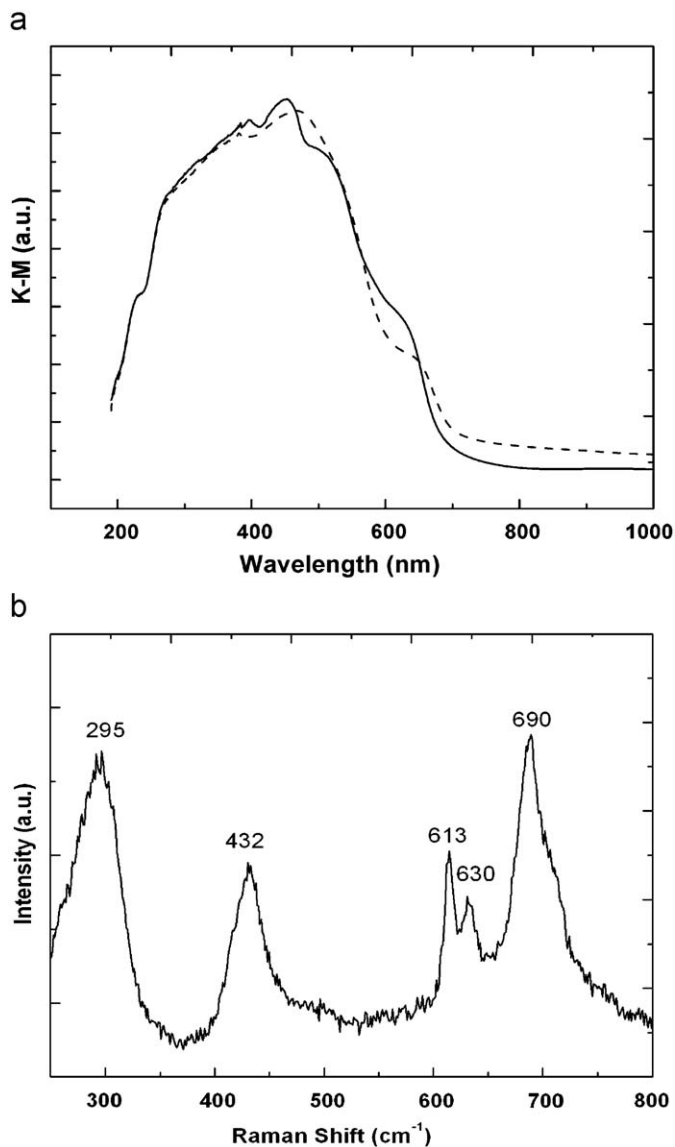


Fig. 7. (a) UV-vis diffuse reflectance spectrum of  $\beta$ -NaFeO<sub>2</sub> (—) and  $\beta$ -AgFeO<sub>2</sub> (-----) and (b) Raman spectrum of  $\beta$ -AgFeO<sub>2</sub>.

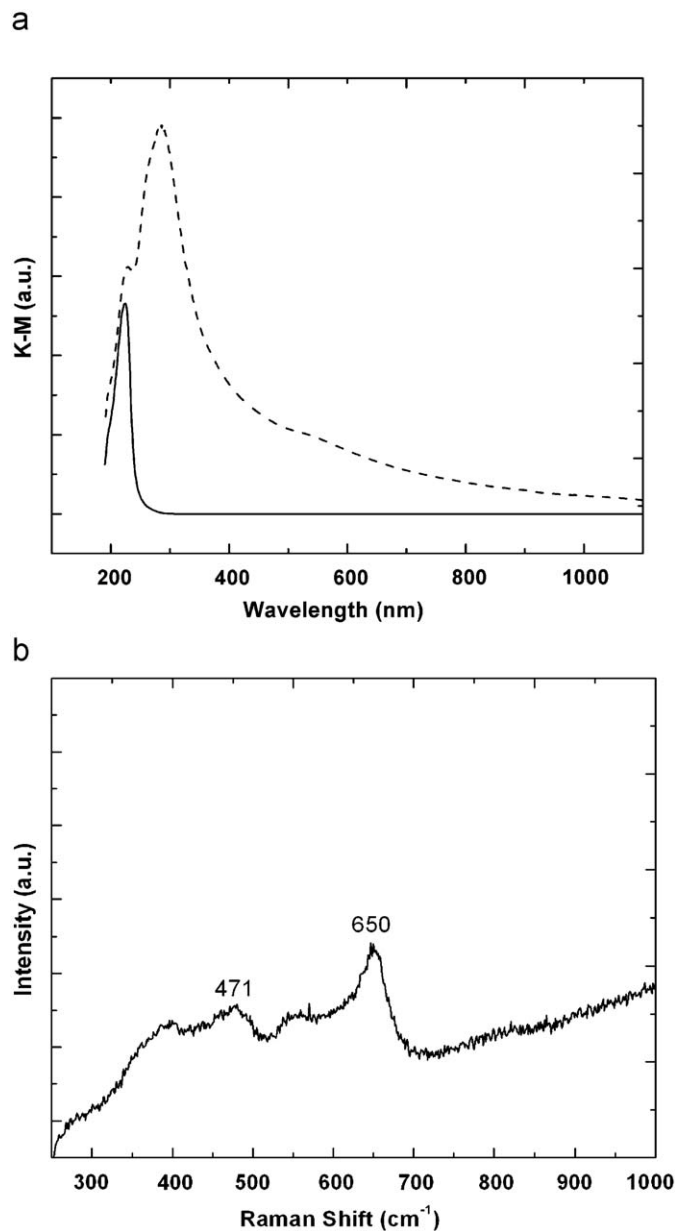


Fig. 9. (a) UV-vis diffuse reflectance spectrum of  $\beta$ -NaGaO<sub>2</sub> (—) and  $\alpha$ -AgGaO<sub>2</sub> (-----) and (b) Raman spectrum of  $\alpha$ -AgGaO<sub>2</sub>.

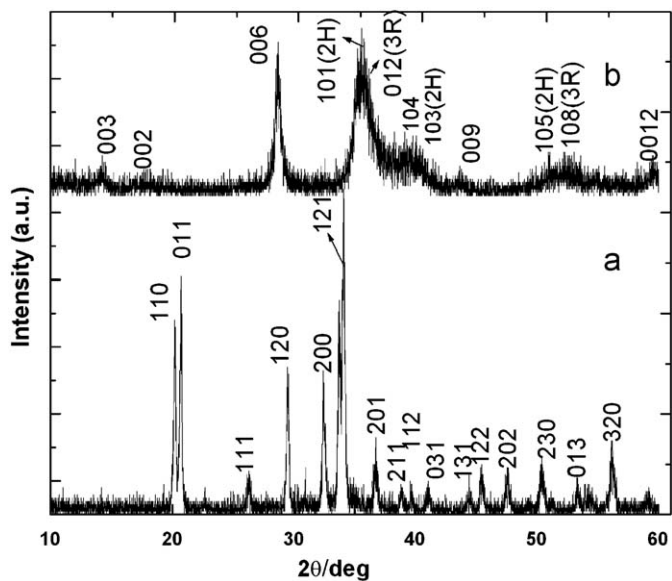


Fig. 8. Powder X-ray diffraction pattern of: (a)  $\beta$ -NaGaO<sub>2</sub> and (b)  $\alpha$ -AgGaO<sub>2</sub>.

#### 4. Conclusions

The present study has clearly demonstrated the advantage of utilizing ultrasound in the synthesis of  $\alpha$ -AgFeO<sub>2</sub> from the hydroxides of silver and iron. Its important role in enhancing the kinetics of the ion-exchange reactions of  $\beta$ -NaMO<sub>2</sub> ( $M = \text{Fe, Ga}$ ) with aqueous AgNO<sub>3</sub>, to generate  $\beta$ -AgFeO<sub>2</sub> and  $\alpha$ -AgGaO<sub>2</sub>, respectively, has been established. All these reactions carried out at room temperature in an open system were very rapid. This method of synthesis is very simple and elegant compared with the ones that exist in the literature. Similar reactions in case of copper were not successful because of the fact that the Cu<sup>+</sup> ion can disproportionate easily. Preliminary investigations indicated that  $\alpha$ -AgGaO<sub>2</sub> (0.15 g) decomposed methylene blue solution (15  $\mu\text{mol/l}$ ) under UV (Philips make 125 W power) irradiation. Detailed studies on these compounds as photocatalysts are underway and will be published elsewhere.

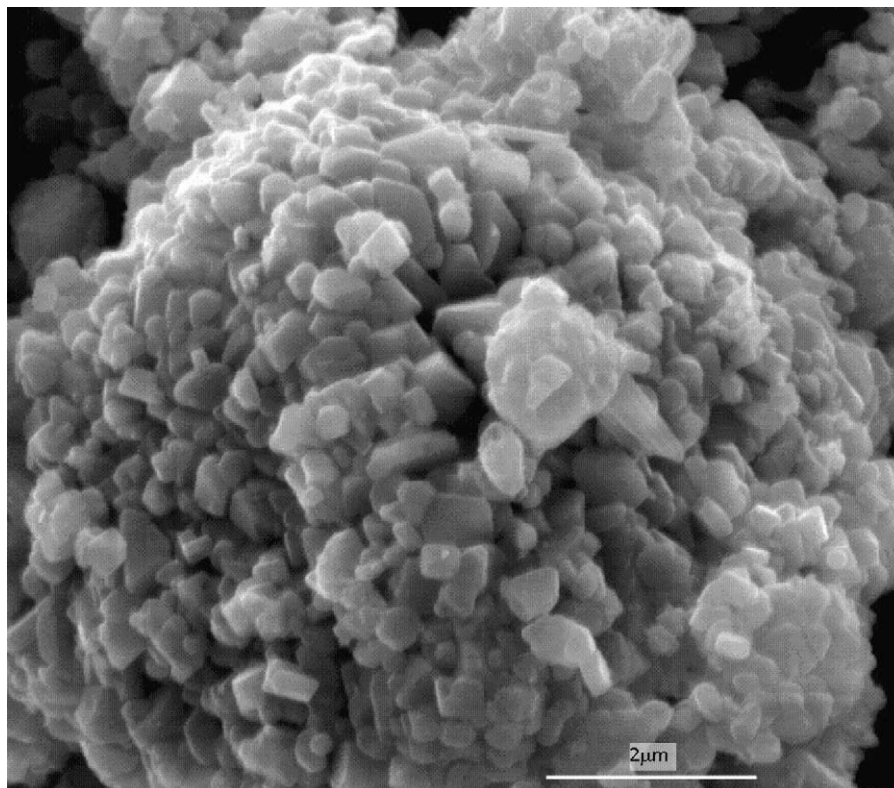


Fig. 10. SEM image of  $\alpha$ -AgGaO<sub>2</sub>.

## Acknowledgments

The authors would like to record their sincere thanks to DST, Government of India and University of Delhi for the financial support to carry out this work. Also thanks are due to Dr. S. Uma for very useful discussions and sharing some experimental facilities for carrying out this work. The authors thank Miss Vaishali Thakral for performing the initial photocatalytic experiments.

## References

- [1] R.D. Shannon, D.B. Rogers, C.T. Prewitt, *Inorg. Chem.* 10 (1971) 713–718.
- [2] C.T. Prewitt, R.D. Shannon, D.B. Rogers, *Inorg. Chem.* 10 (1971) 719–723.
- [3] D.B. Rogers, R.D. Shannon, C.T. Prewitt, J.L. Gilson, *Inorg. Chem.* 10 (1971) 723–727.
- [4] V.E. Thilo, W. Gessner, *Z. Anorg. Allg. Chem.* 345 (1966) 151–164.
- [5] V.W. Gessner, *Z. Anorg. Allg. Chem.* 360 (1968) 247–258.
- [6] F.A. Benko, F.P. Koffyberg, *J. Phys. Chem. Solids* 45 (1984) 57–59.
- [7] F.A. Benko, F.P. Koffyberg, *Can. J. Phys.* 63 (1985) 1306–1308.
- [8] F.A. Benko, F.P. Koffyberg, *J. Phys. Status Solidi A* 94 (1986) 231–234.
- [9] F.A. Benko, F.P. Koffyberg, *J. Phys. Chem. Solids* 48 (1987) 431–434.
- [10] H. Kawazoe, M. Yasukawa, H. Hyodo, M. Kurita, H. Yanagi, H. Hosono, *Nature* 389 (1997) 939–942.
- [11] R. Nagarajan, N. Duan, M.K. Jayaraj, J. Li, K.A. Vanaja, A. Yokochi, A. Draeseke, J. Tate, A.W. Sleight, *Int. J. Inorg. Mater.* 3 (2001) 265–270.
- [12] R. Nagarajan, S. Uma, M.K. Jayaraj, J. Tate, A.W. Sleight, *Solid State Sci.* 4 (2002) 787–792.
- [13] W.C. Sheets, E.S. Stampler, M.I. Bertoni, M. Sasaki, T.J. Marks, T.O. Mason, K.R. Poeppelmeier, *Inorg. Chem.* 47 (2008) 2696–2705.
- [14] W.C. Sheets, E. Mugnier, A. Barnabe, T.J. Marks, K.R. Poeppelmeier, *Chem. Mater.* 18 (2006) 7–20.
- [15] A. Krause, S. Gawryck, *Z. Anorg. Allg. Chem.* 238 (1938) 406–412.
- [16] K.S. Suslick, *Science* 247 (1990) 1439–1445.
- [17] A. Gedanken, *Ultrasonics Sonochemistry* 11 (2004) 47–55.
- [18] T.J. Mason, *Ultrasonics* 24 (1986) 245–253.
- [19] K.H. Kim, K.B. Kim, *Ultrasonics Sonochemistry* 15 (2008) 1019–1025.
- [20] Y. Maruyama, H. Irie, K. Hashimoto, *J. Phys. Chem. B* 110 (2006) 23274–23278.
- [21] Y. Takeda, J. Akkagi, A. Edagawa, M. Inagaki, S. Naka, *Mater. Res. Bull.* 15 (1980) 1167–1172.
- [22] S.Y. Zheng, G.S. Jiang, J.R. Su, C.F. Zhu, *Mater. Lett.* 60 (2006) 3871–3873.
- [23] H. Takatsu, S. Yonezawa, S. Mouri, S. Nakatsuji, K. Tanaka, Y. Maeno, *J. Phys. Soc. Jpn.* 76 (2007) 104701.
- [24] P. Bruesch, C. Schuler, *J. Phys. Chem. Solids* 32 (1971) 1025–1038.
- [25] G. Hakvoort, *Therm. Anal.* 1 (1974) 469–477.
- [26] S. Ouyang, H. Zhang, D. Li, T. Yu, J. Ye, Z. Zou, *J. Phys. Chem. B* 110 (2006) 11677–11682.
- [27] H. Kabelka, H. Kuzmany, P. Krempf, *Solid State Commun.* 27 (1978) 1159–1162.
- [28] E.B. Flint, K.S. Suslick, *Science* 253 (1991) 1397–1399.
- [29] K. Chatakondur, M.L.H. Green, M.E. Thompson, K.S. Suslick, *J. Chem. Soc. Chem. Commun.* (1987) 900–901.
- [30] T. Lepoint, F. Mullie, *Ultrasonics Sonochemistry* 1 (1994) S13–S22.
- [31] K.S. Suslick, G.J. Price, *Annu. Rev. Mater. Sci.* 29 (1999) 295–326.
- [32] L.C. Hagenson, L.K. Doraiswamy, *Chem. Eng. Sci.* 53 (1998) 131–148.